

Electronic Supporting Information

Peritectic Phase Transition of Benzene and Acetonitrile into a Cocrystal Relevant to Titan, Saturn's Moon

Christina A. McConville,^a Yunwen Tao,^a Hayden A. Evans,^b Benjamin A. Trump,^b Jonathan B. Lefton,^a Wenqian Xu,^c Andrey A. Yakovenko,^c Elfi Kraka,^a Craig M. Brown^{b,d} and Tomče Runčevski*^a

^a Department of Chemistry, Southern Methodist University, Dallas, TX 75275 (USA) E-mail: truncevski@smu.edu.

^b National Institute of Standards and Technology, Center for Neutron Research, Gaithersburg, MD 20899 (USA).

^c X-ray Science Division, Advanced Photon Source, Argonne National Laboratory, Argonne, IL 60439 (USA).

^d Department of Chemical and Biomolecular Engineering, University of Delaware, DE 19716 (USA).

Contents

1. Notes and Acknowledgements	1
2. Differential scanning calorimetry and phase diagram.....	2
Figure S1. DSC curves of acetonitrile and benzene mixtures	3
Figure S2. Comparison of the phase diagram with earlier data.	5
3. Powder X-ray data collection.....	6
4. Crystal structure solution and refinement	6
Table S1. Crystallographic data of the 1:3 acetonitrile:benzene cocrystal.....	7
Figure S3. Rietveld refinement plot at 100 K.	8
Figure S4. Rietveld refinement plot at 251 K.	9
Figure S5. Crystal packing of the benzene cocrystals with acetonitrile and ethane.....	10
5. Computational details	11
Figure S6. Optimized geometry of the (acetonitrile) ₂ (benzene) ₁₂ cluster.	11
Figure S7. Crystal packing of the 1:3 acetonitrile:benzene cocrystal overlaid with the optimized cluster.	11
6. Thermal expansion	12
Figure S8. Pawley fitting of the diffraction data collected at 100 K.....	12
Figure S9. Pawley fitting of the diffraction data collected upon cooling.....	13
Figure S10. Pawley fitting of the diffraction data collected upon heating.	13
Figure S11. Thermal expansion properties of the 1:3 acetonitrile:benzene cocrystal (on cooling).	14
Figure S12. Thermal expansion properties of the 1:3 acetonitrile:benzene cocrystal (on heating).....	15
Table S2. Changes of the unit cell parameters upon cooling of the 1:3 acetonitrile:benzene cocrystal.	16
Table S3. Changes of the unit cell parameters upon cooling of benzene.....	17
Table S4. Changes of the unit cell parameters upon heating of the 1:3 acetonitrile:benzene cocrystal.	18
Table S5. Changes of the unit cell parameters upon heating of benzene	19
References	20

1. Notes and Acknowledgements

T.R. and C.A.M. thank the Robert A. Welch Foundation (Grant No.: N-2012-20190330) for financial support. C.A.M. thanks the Texas Space Grant Consortium graduate fellowship. H.A.E. thanks the National Research Council (USA) for financial support through the Research Associate Program. We thank SMU for providing generous computational resources. This research used Beamline 17-BM at the Advanced Photon Source, a U.S. Department of Energy (DOE) Office of Science User Facility operated for the DOE Office of Science by Argonne National Laboratory under Contract No. DE-AC02-06CH11357.

Certain commercial equipment, instruments, or materials are identified in this document. Such identification does not imply recommendation or endorsement by the National Institute of Standards and Technology, nor does it imply that the products identified are necessarily the best available for the purpose.

2. Differential scanning calorimetry and phase diagram

Acetonitrile:benzene mixtures with varying molar ratios were prepared by measuring calculated amounts of acetonitrile (VWR, $\geq 99.95\%$) and benzene (Millipore, $\geq 99.8\%$) into 2mL tared GCMS vials with Teflon septa (for compatibility with benzene). The vials were mixed via vigorous shaking for 1 min, and an aliquot of the sample was pipetted into an aluminum DSC pan (30 μL , 99.5% purity) such that the mass of the sample was $5.0\text{mg} \pm 0.5\text{mg}$. Each pan was hermetically sealed using a sealing press and thermal analysis was conducted on the samples using Differential Scanning Calorimetry (DSC) instrument (Netzsch DSC 214 Polyma with ASC). The samples were cooled from room temperature to 100K using a CC 200 F3 Cooling Device (Netzsch) equipped with liquid nitrogen at a rate of 2K/min to match the cooling rate used during synchrotron measurements. Nitrogen (Matheson Tri-Gas) was used for both the purge gas and protective gas sources, at rates of 40 ml/min and 60ml/min, respectively. The DSC curves (Figure S1) were exported using the Netzsch DSC software (Proteus® Version 7.1.0) and analyzed using the Python-based libraries Matplotlib and SciPy. The temperatures of each phase transition were assumed to be the temperature at the location of the peak in the DSC data; these points were located using the agreextrema function from the signal processing package SciPy.signal. The function was used to locate the relative minima of the DSC melting curve for each molar ratio, and the temperature values corresponding to each minima were plotted versus molar ratio. Peaks determined to be due to ice buildup in the sample chamber during humid conditions were excluded from the data. To construct the phase diagram, best-fit lines were determined from each group of data points corresponding to a particular transition using the Polyfit and polyval functions of the polynomial module within the Python-based library NumPy. The upper fusion boundary line (f), eutectic line (e), solid-to-solid transition line from the β phase to the α phase of acetonitrile (t), and peritectic boundary line (p) were determined using linear fits, and the lower fusion boundary line was determined using a 2nd order polynomial fit.

Data from previous studies^{S1,S2} on the acetonitrile-benzene system were also plotted alongside our data for comparison (Figure S2). The main discrepancies lie in the slope of the upper fusion boundary line and in the existence of an additional transition line around 216 K, both of which can be explained by the differences between the experimental methods used. In both previous studies, a freezing point apparatus was used to determine transition temperatures, requiring that the recorded transition temperature be the onset temperature of that transition, while our method of using DSC allowed us to quantify the transition and locate the peak temperature; specifically, because the transitions for benzene are relatively broad and span several degrees, this results in an expected deviation in temperatures within the upper fusion boundary line. Additionally, the use of a freezing point apparatus would not allow for the observation of solid-to-solid transitions, whereas DSC allows for the detection of these transitions with exceptional detail; as such, we observe a transition line from the β phase to the α phase of acetonitrile where previous studies do not.

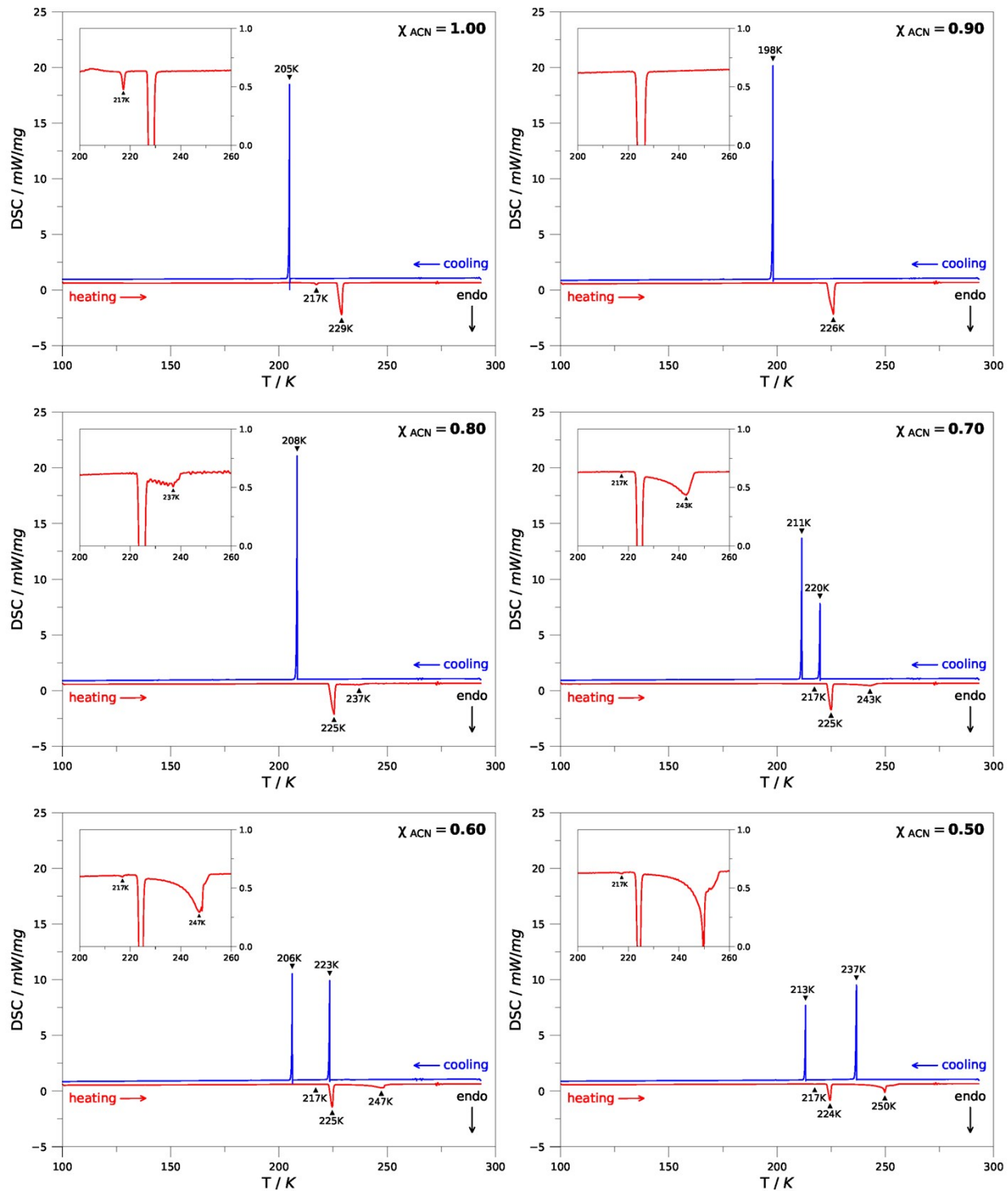
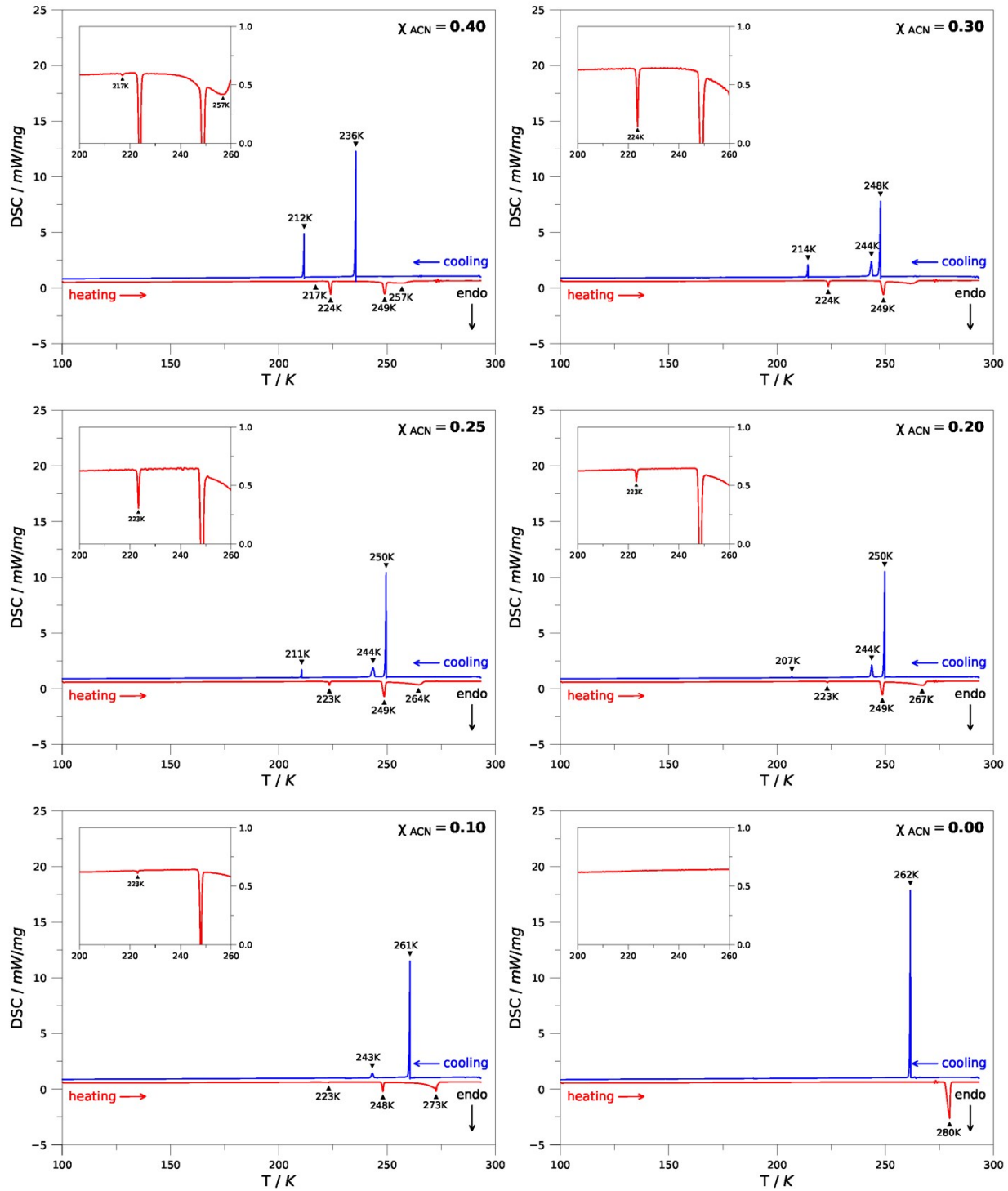


Figure S1. DSC curves of acetonitrile and benzene mixtures

Cooling and heating curves presented in blue and red, respectively. (continued)



(continued)

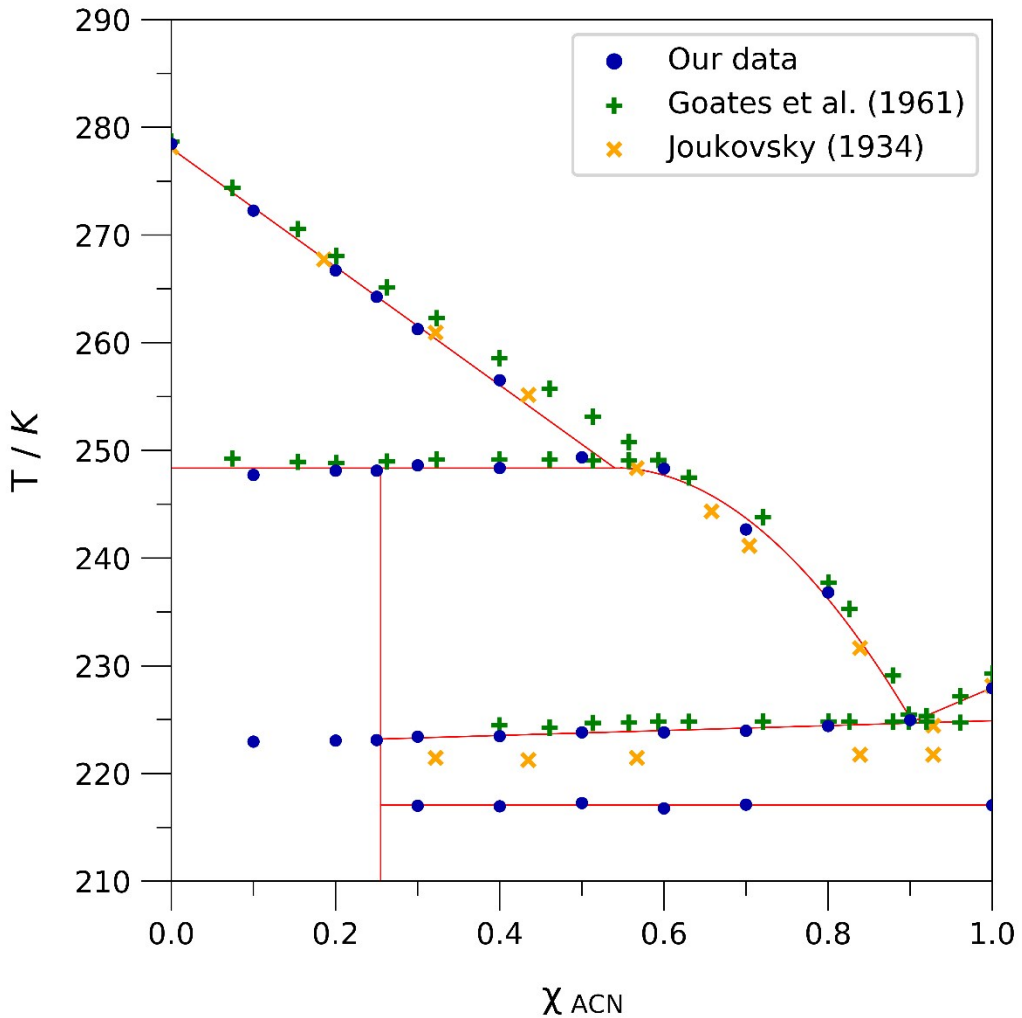


Figure S2. Comparison of the phase diagram with earlier data.

The measured DSC data are plotted as blue dots, whereas data from references S1 and S2 are plotted as yellow exes and green crosses, respectively.

3. Powder X-ray data collection

In situ powder X-ray diffraction (PXRD) data on a 1:3 mixture of acetonitrile:benzene was collected on Beamline 17-BM at the Advanced Photon Source at Argonne National Laboratory. Measured amount of the liquids were mixed together and put in kapton capillaries. The capillaries were rotated for better particles statistics. An Oxford Cryosystems Cryostream 800 was used to maintain the temperature of the sample. Scattered intensity was measured by a PerkinElmer a-Si flat panel detector. Data was simultaneously collected from room temperature to 100 K with heating cooling rate of 2 K/min. The average wavelength of measurement was 0.2409 Å.

For the gas dosing experiments, the capillary was attached to a custom designed gas-dosing cell equipped with a gas valve and transferred to the goniometer head. All adsorbed air was then removed by evacuating *in situ* using a turbomolecular pump. After evacuation, ethane was introduced into the system. An Oxford Cryosystems Cryostream 800 was used to maintain the temperature of the sample. Scattered intensity was measured by a PerkinElmer a-Si flat panel detector. The average wavelength of measurement was 0.4525 Å.

4. Crystal structure solution and refinement

The PXRD data collected *in situ* before and after the peritectic transition are amenable to structural analyses. In the temperature window from 245 K to 263 K only reflections of benzene were observed. We selected the pattern collected at 251 K as representative set for data analysis. Using these data, we performed Rietveld refinement^{S3} on the crystal structure of the *Pbca* modification of benzene.^{S4} All of the reflections in the pattern were accounted for during the refinement. The final Rietveld plots before and after the peritectic transition are presented in Figure S3 and S4; details of the refinement are given in Table S1.

At temperatures below 245 K, reflection of an unknown crystalline phase were observed, in addition to reflection from the *Pbca* modification of benzene.^{S4} The reflections of benzene were accounted for by a Rietveld refinement^{S3} of the known structure.^{S4} The uncounted reflections were used to solve the crystal structure of the unknown phase. The diffraction peaks of the new phase were indexed by a singular value decomposition function,^{S5} as implemented in TOPAS-6 (Coelho Software, 2018). The indexing led to a trigonal, *R*-centred unit cell which parameters were refined by Pawley fitting.^{S6} The analysis of systematic absences indicated either $\bar{3}$ or $\bar{3}m$ Laue class. The volume and shape of the asymmetric unit indicated to 1 to 3 composition of acetonitrile and benzene and presence of a 3-fold axis. Considering the asymmetry of acetonitrile, *R*3 was chosen as best candidate. Crystal structure solution was initiated using the approach of simulated annealing,^{S7} with fixed position of acetonitrile (used to define the origin of the polar space group) and freely rotated and translated benzene. To account for preferred orientation, sixth-order spherical harmonic model was included.^{S8} The crystal structure and composition of the peritectic product, 1:3 acetonitrile:benzene, was confirmed by a Rietveld refinement.^{S3} The final Rietveld plots before and after peritectic transition are presented in Figure 2 in the main text; details of the refinement are given in Table S1.

Table S1. Crystallographic data of the 1:3 acetonitrile:benzene cocrystal.

Experimental, unit cell, and refinement parameters obtained by Rietveld refinement using X-ray powder diffraction patterns of 1:3 mixture of acetonitrile and benzene, collected at 100 K and 251 K. Values in parentheses indicate one standard deviation.

	1:3 acetonitrile:benzene	benzene	benzene
λ (Å)		0.2409	
2θ range (°)		1 – 8	
T (K)	100 K		251 K
Space Group	<i>R</i> 3	<i>Pbca</i>	<i>Pbca</i>
<i>a</i> (Å)	15.893(3)	7.370(2)	7.4757(6)
<i>b</i> (Å)	15.893(3)	9.449(3)	9.642(2)
<i>c</i> (Å)	5.7203(10)	6.817(2)	7.0134(9)
<i>V</i> (Å ³)	1251.4(10)	474.8(1)	505.5(1)
Weight %	79.1(7)	20.9(7)	100
<i>R</i> _{wp} (%) ^a	5.90		3.62
<i>R</i> _{exp} (%) ^a	0.02		0.02
<i>R</i> _p (%) ^a	4.43		2.51
No. parameters	53		40

^a As defined in TOPAS-6

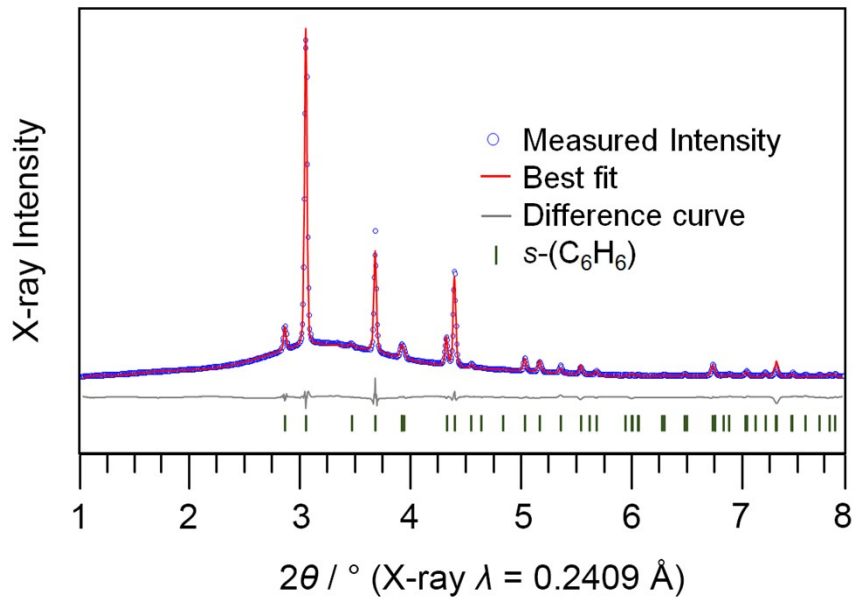


Figure S3. Rietveld refinement plot at 100 K.

The collected diffraction data is presented as open circles, the simulated pattern is presented as red line and the difference pattern as a gray line.

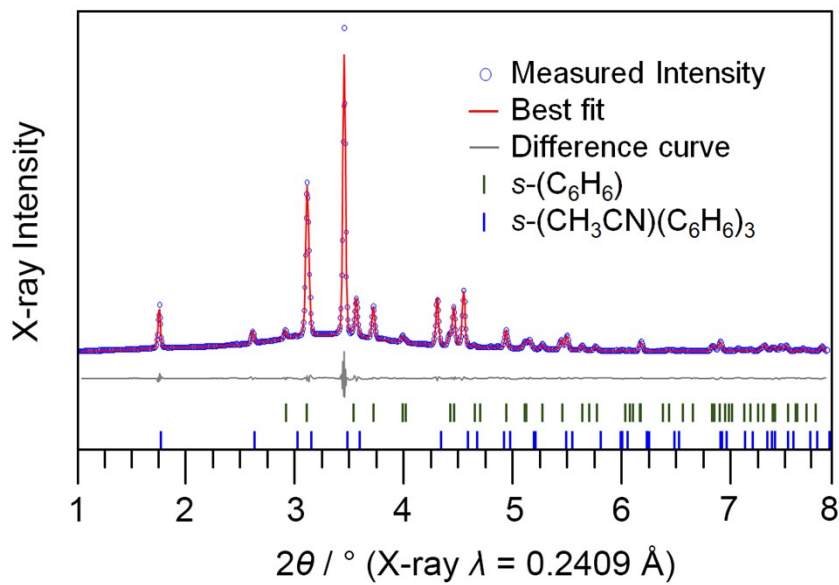


Figure S4. Rietveld refinement plot at 251 K.

The collected diffraction data is presented as open circles, the simulated pattern is presented as red line and the difference pattern as a gray line.

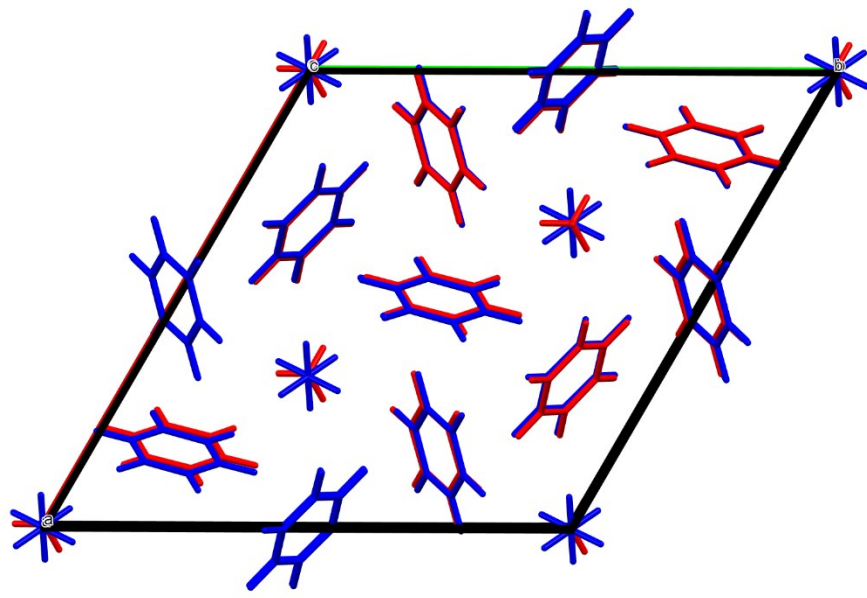


Figure S5. Crystal packing of the benzene cocrystals with acetonitrile and ethane.

The crystal structure 1:3 acetonitrile:benzene is presented in red, whereas the crystal structure of the 1:3 ethane:benzene cocrystal⁵⁹ is presented in blue.

5. Computational details

Both $(\text{acetonitrile})_2(\text{benzene})_{12}$ clusters were optimized with PBE pure density functional^{S10} with Pople's 6-31G(d,p) basis set.^{S11} The dispersion interaction was included via Grimme's empirical D3 correction with Becke-Johnson damping.^{S12} The vibrational analysis performed at the same level of theory confirmed that the structure is a local minimum on the potential energy surface. The calculation was conducted with Gaussian 16 package^{S13} with a pruned (99,590) DFT grid.

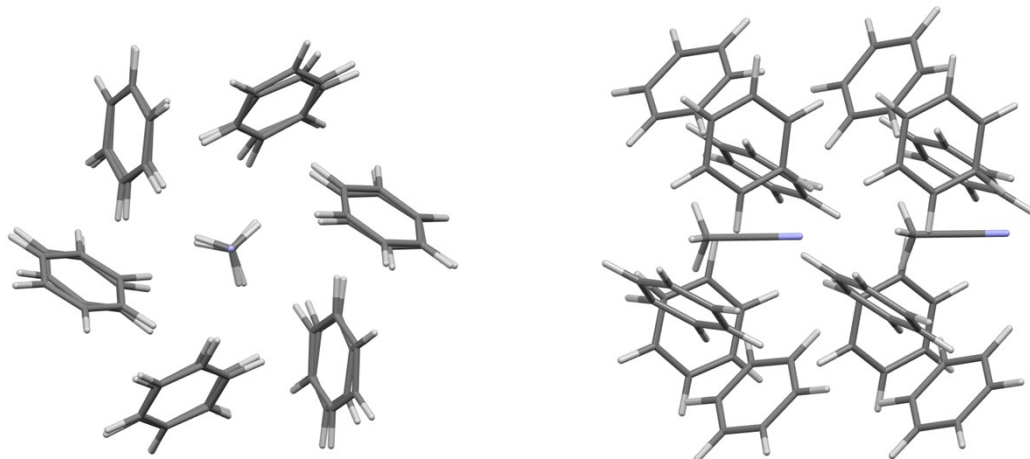


Figure S6. Optimized geometry of the $(\text{acetonitrile})_2(\text{benzene})_{12}$ cluster.

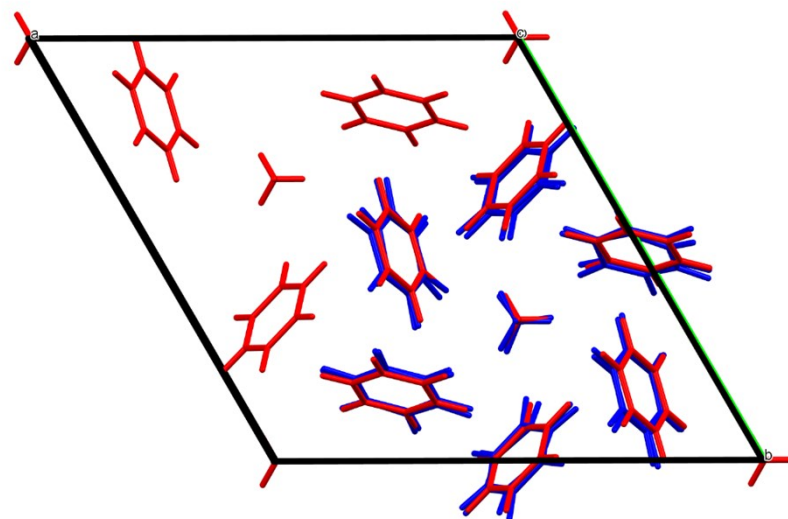


Figure S7. Crystal packing of the 1:3 acetonitrile:benzene cocrystal overlaid with the optimized cluster.

The crystal structure 1:3 acetonitrile:benzene is presented in red, whereas the relative atomic positions of the optimized $(\text{acetonitrile})_2(\text{benzene})_{12}$ cluster are presented in blue.

6. Thermal expansion

The thermal expansion properties of the 1:3 acetonitrile:benzene cocrystal were studied by observing the changes of the unit cell parameters upon cooling and heating. For obtaining accurate unit cell parameters, Pawley fitting^{S6} was performed against the collected data (Figures S6-S8). The fitted parameters are given in Tables S2-S5.

The thermal expansion properties were calculated using the PASCal software.^{S14} The expansivity indicatrix and plots of the fitted data are given in Figures S9 and S10.

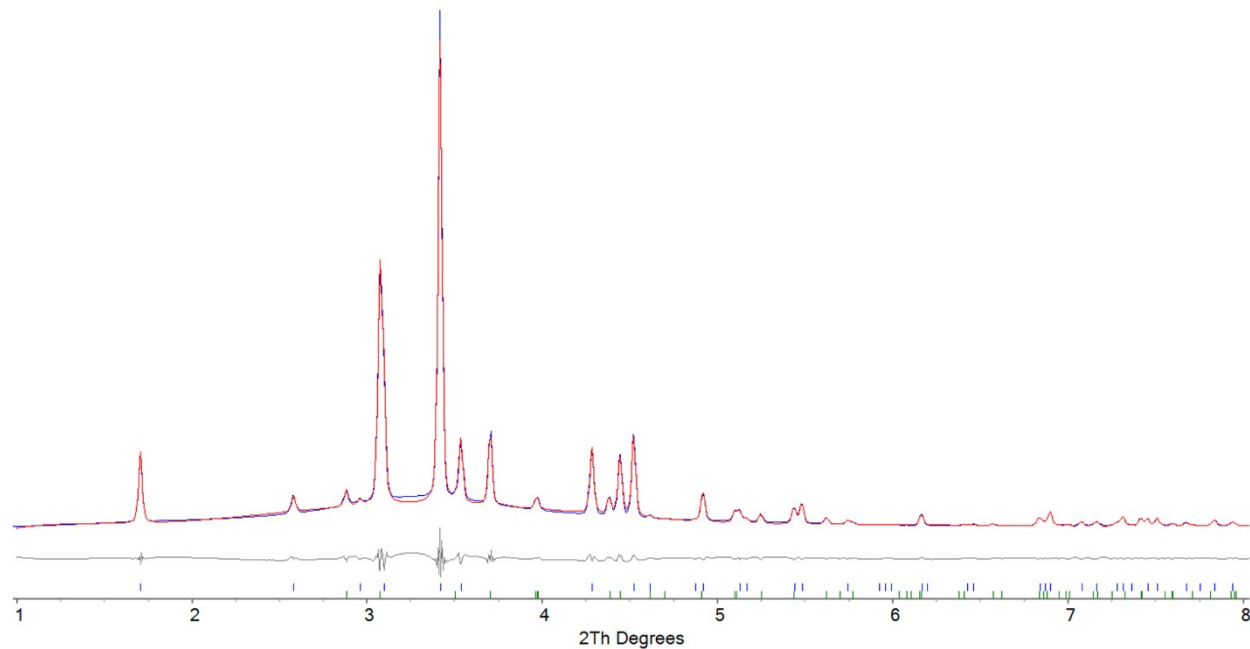


Figure S8. Pawley fitting of the diffraction data collected at 100 K.

Bragg reflections of the 1:3 acetonitrile:benzene cocrystal and solid benzene are presented in blue and green color, respectively. The collected data is presented as blue line. The fitted and difference curves are presented in red and grey, respectively.

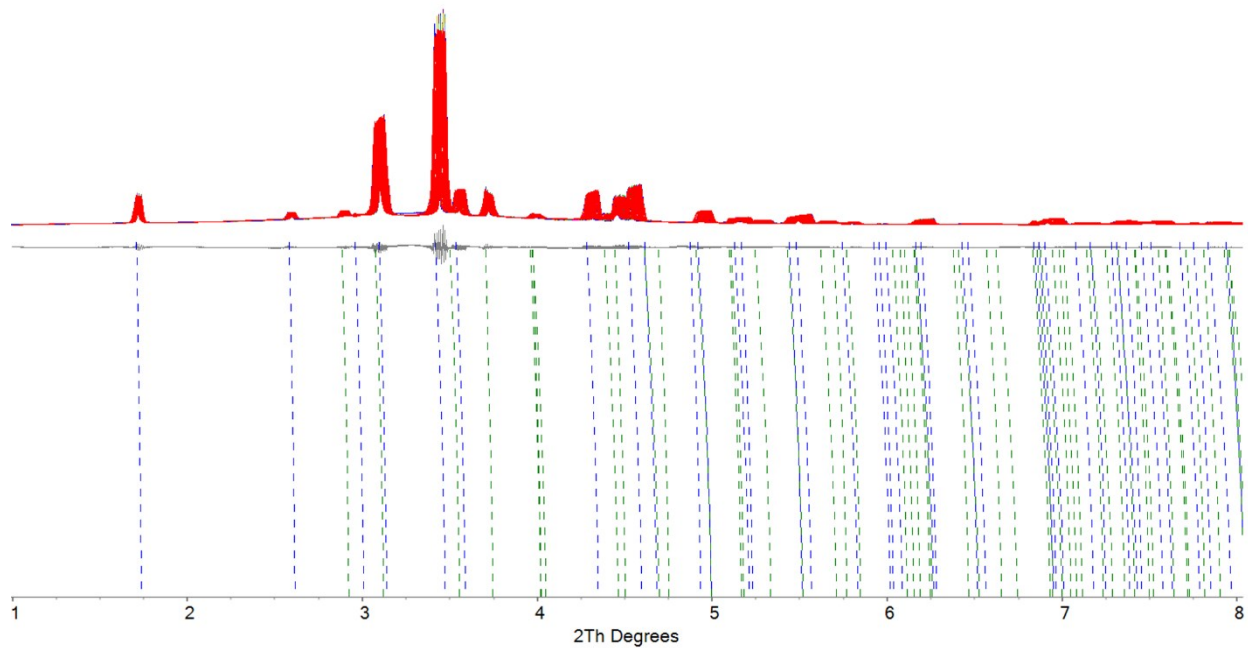


Figure S9. Pawley fitting of the diffraction data collected upon cooling.

Bragg reflections of the 1:3 acetonitrile:benzene cocrystal and solid benzene are presented in blue and green color, respectively. The fitted and difference curves are presented in red and grey, respectively.

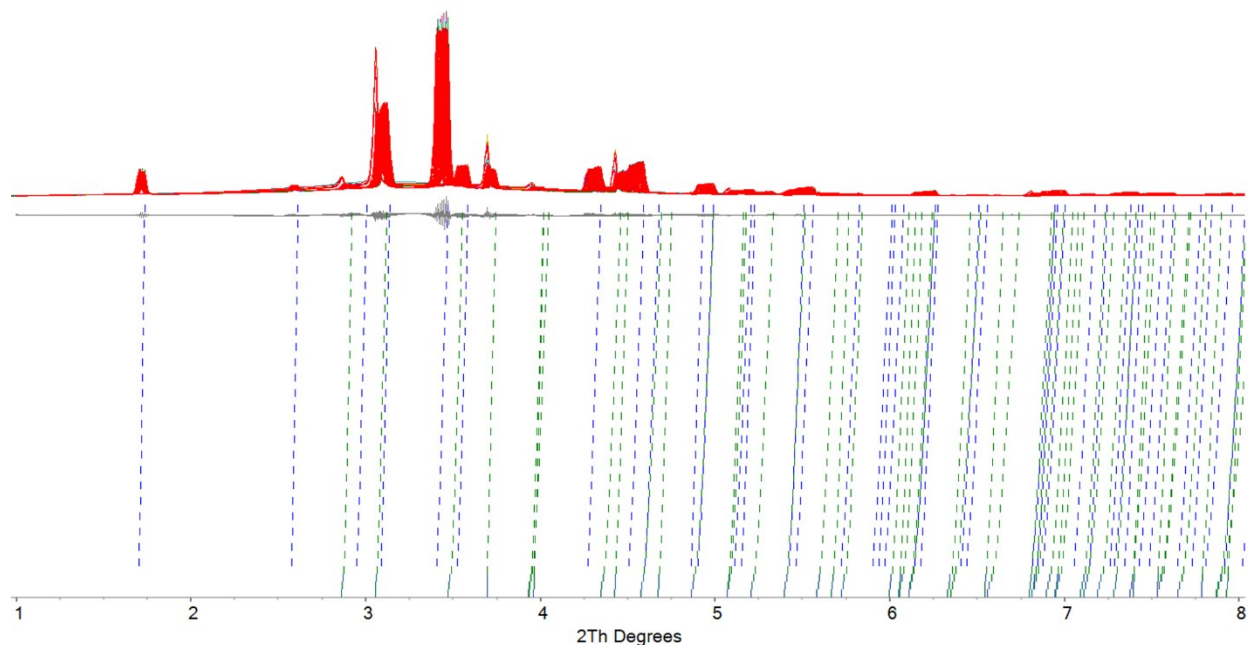


Figure S10. Pawley fitting of the diffraction data collected upon heating.

Bragg reflections of the 1:3 acetonitrile:benzene cocrystal and solid benzene are presented in blue and green color, respectively. The fitted and difference curves are presented in red and grey, respectively.

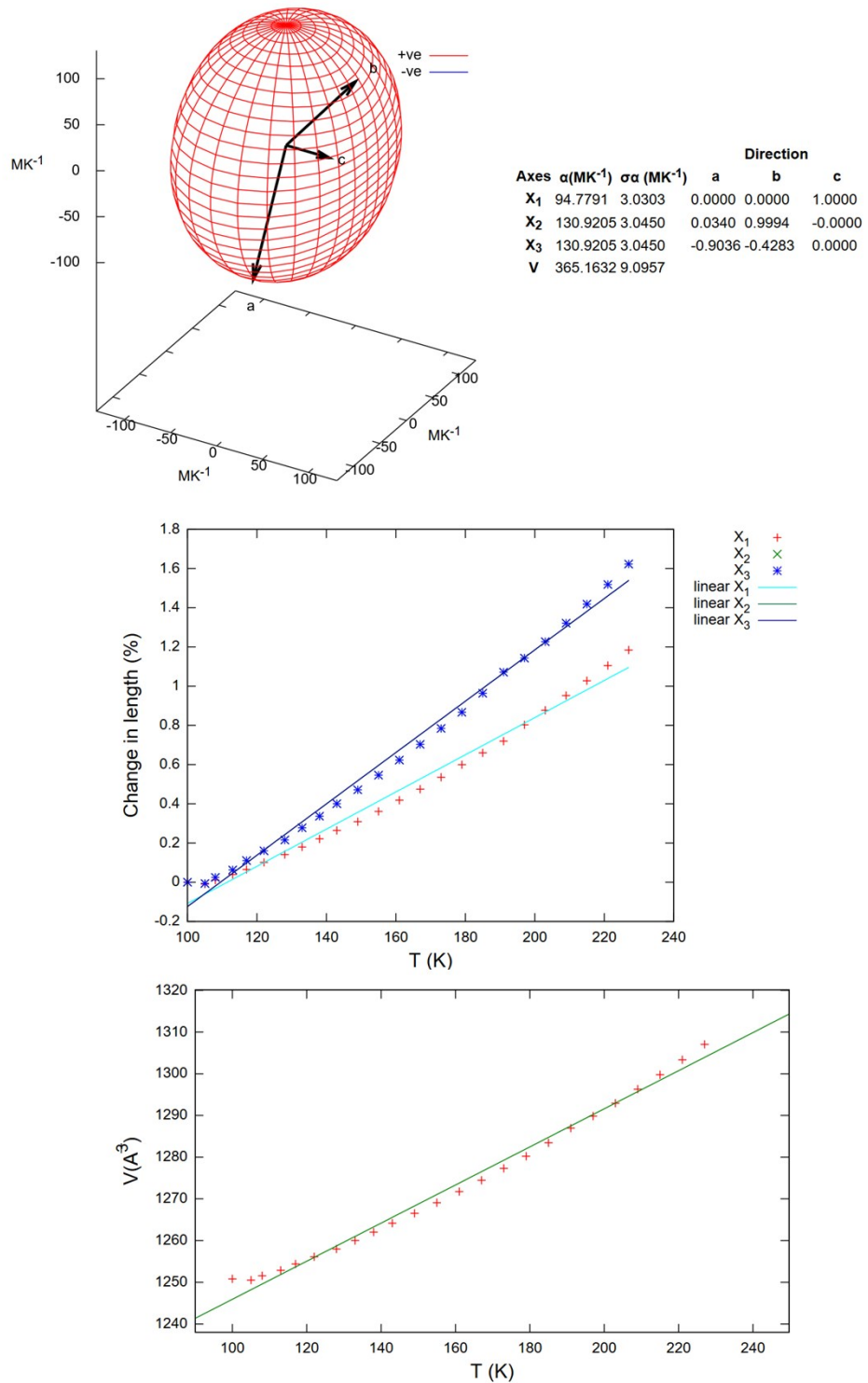


Figure S11. Thermal expansion properties of the 1:3 acetonitrile:benzene cocrystal (on cooling).

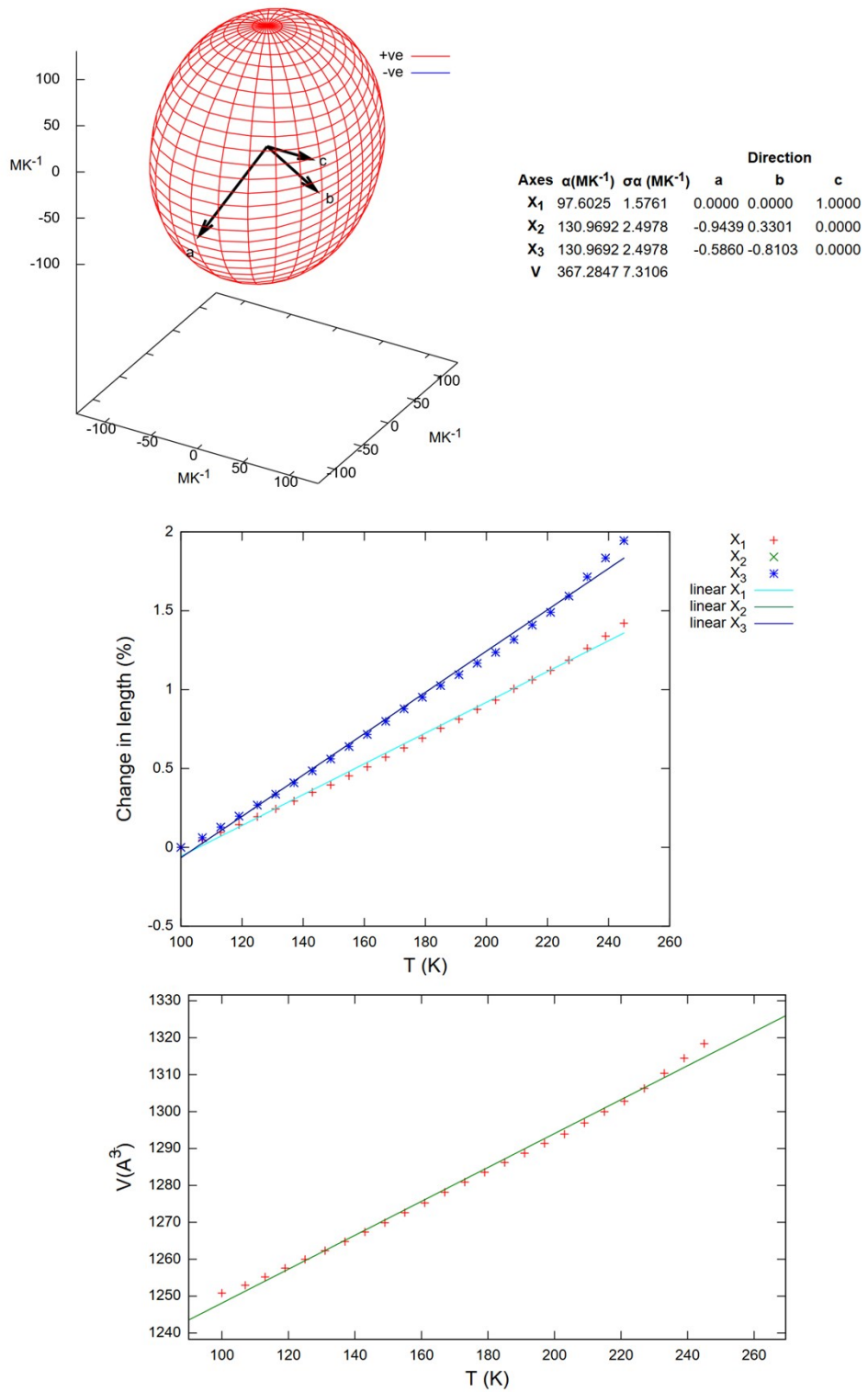


Figure S12. Thermal expansion properties of the 1:3 acetonitrile:benzene cocrystal (on heating).

Table S2. Changes of the unit cell parameters upon cooling of the 1:3 acetonitrile:benzene cocrystal.

The values and errors are obtained by a Pawley fitting^{S6} against the experimental data.

T (K)	a (Å)	error	c (Å)	error	V (Å ³)	error
227	16.15296	0.003488	5.784329	0.001294	1307.037	0.636
221	16.13636	0.000395	5.779837	0.000794	1303.339	0.19
215	16.12046	0.00039	5.775403	0.000782	1299.774	0.187
209	16.10496	0.000369	5.771079	0.000738	1296.304	0.176
203	16.08999	0.000351	5.766759	0.0007	1292.927	0.167
197	16.07669	0.000343	5.762516	0.000694	1289.84	0.165
191	16.06528	0.000339	5.757776	0.000686	1286.952	0.163
185	16.04814	0.000339	5.754368	0.000687	1283.446	0.163
179	16.03279	0.000345	5.750932	0.000701	1280.227	0.166
173	16.01961	0.000351	5.747244	0.000716	1277.304	0.169
167	16.00668	0.000348	5.743773	0.000704	1274.472	0.166
161	15.99405	0.000344	5.740571	0.000696	1271.752	0.164
155	15.98176	0.000341	5.737294	0.000686	1269.073	0.161
149	15.9699	0.000335	5.734297	0.000671	1266.529	0.158
143	15.95864	0.000351	5.731744	0.000691	1264.18	0.162
138	15.94847	0.000364	5.729284	0.000705	1262.029	0.166
133	15.93906	0.000371	5.726916	0.000718	1260.017	0.169
128	15.92923	0.000384	5.724709	0.000741	1257.98	0.174
122	15.92049	0.00039	5.722442	0.000755	1256.102	0.177
117	15.91254	0.000394	5.72036	0.000756	1254.391	0.177
113	15.90493	0.000389	5.718919	0.000747	1252.876	0.175
108	15.89885	0.000372	5.717282	0.000714	1251.559	0.167
105	15.89392	0.00037	5.716129	0.000709	1250.532	0.166
100	15.894974	0.000244	5.716647	0.000486	1250.811	0.113

Table S3. Changes of the unit cell parameters upon cooling of benzene

The values are obtained by a Pawley fitting^{S6} against the experimental data.

T (K)	a (Å)	error	b (Å)	error	c (Å)	error	V (Å ³)	error
227	7.45177	0.001659	9.572391	0.003445	6.950154	0.001842	495.763	0.248
221	7.447224	0.000587	9.561917	0.002871	6.940802	0.001411	494.253	0.183
215	7.442754	0.000583	9.553471	0.00286	6.931212	0.001405	492.838	0.182
209	7.438184	0.000566	9.545035	0.002745	6.922448	0.001351	491.478	0.175
203	7.433646	0.00054	9.537382	0.002617	6.914095	0.001289	490.192	0.166
197	7.430347	0.000534	9.530287	0.002604	6.905505	0.001291	489.002	0.166
191	7.42913	0.000529	9.521856	0.002509	6.895438	0.001274	487.777	0.161
185	7.421858	0.000538	9.514	0.0025	6.888959	0.001277	486.44	0.16
179	7.41569	0.000548	9.50608	0.002445	6.88314	0.001247	485.221	0.157
173	7.411298	0.000546	9.498203	0.002458	6.876556	0.001146	484.068	0.153
167	7.406664	0.000546	9.492059	0.002491	6.870631	0.001106	483.036	0.153
161	7.402226	0.000543	9.486602	0.002492	6.864786	0.001064	482.059	0.151
155	7.397848	0.000542	9.48102	0.002498	6.859166	0.001052	481.096	0.151
149	7.393678	0.000539	9.475354	0.002507	6.853945	0.001052	480.172	0.151
143	7.389648	0.000563	9.472406	0.002731	6.847835	0.001185	479.333	0.165
138	7.385975	0.000586	9.46864	0.002872	6.842885	0.001256	478.558	0.174
133	7.382608	0.0006	9.464245	0.002887	6.838603	0.001274	477.819	0.175
128	7.37957	0.000615	9.460796	0.00297	6.833524	0.001297	477.093	0.179
122	7.376542	0.00063	9.457171	0.003029	6.829344	0.001315	476.423	0.183
117	7.373706	0.000637	9.453959	0.003075	6.825554	0.001333	475.814	0.185
113	7.371073	0.000635	9.449571	0.003027	6.822749	0.001318	475.228	0.182
108	7.368995	0.000608	9.448451	0.002899	6.819302	0.001262	474.798	0.175
105	7.367327	0.000606	9.446284	0.002893	6.817128	0.001259	474.43	0.174
100	7.367604	0.000389	9.447755	0.000974	6.817147	0.000665	474.523	0.072

Table S4. Changes of the unit cell parameters upon heating of the 1:3 acetonitrile:benzene cocrystal.

The values and errors are obtained by a Pawley fitting^{S6} against the experimental data.

T (K)	a (Å)	error	c (Å)	error	V (Å ³)	error
100	15.894974	0.000244	5.716647	0.000486	1250.811	0.113
107	15.90469	0.000395	5.719329	0.00076	1252.928	0.178
113	15.91527	0.000394	5.722085	0.000759	1255.2	0.178
119	15.92643	0.000387	5.724842	0.000747	1257.567	0.175
125	15.93748	0.000372	5.727762	0.000717	1259.954	0.168
131	15.94848	0.000364	5.73058	0.000704	1262.315	0.165
137	15.96004	0.000359	5.733458	0.000696	1264.781	0.164
143	15.97205	0.000364	5.736561	0.000716	1267.37	0.168
149	15.98405	0.000368	5.739262	0.000745	1269.874	0.175
155	15.9966	0.00037	5.742561	0.000745	1272.6	0.175
161	16.00871	0.000376	5.745797	0.000759	1275.246	0.179
167	16.02198	0.000374	5.749335	0.000761	1278.146	0.179
173	16.03456	0.000376	5.75269	0.000767	1280.901	0.181
179	16.04626	0.000364	5.756225	0.000739	1283.559	0.175
185	16.05789	0.000329	5.759795	0.000667	1286.219	0.158
191	16.06897	0.000339	5.763112	0.000684	1288.736	0.162
197	16.08049	0.000355	5.766642	0.000715	1291.375	0.17
203	16.09146	0.000366	5.770022	0.000734	1293.895	0.175
209	16.10442	0.00038	5.77413	0.000763	1296.903	0.182
215	16.11895	0.000394	5.777376	0.00079	1299.974	0.189
221	16.13176	0.000391	5.780748	0.000788	1302.802	0.188
227	16.1482	0.000371	5.784493	0.00074	1306.303	0.177
233	16.16748	0.000355	5.788742	0.000704	1310.386	0.169
239	16.18654	0.000346	5.793177	0.000681	1314.485	0.164
245	16.20412	0.000344	5.797872	0.000672	1318.408	0.163

Table S5. Changes of the unit cell parameters upon heating of benzene

The values and errors are obtained by a Pawley fitting^{S6} against the experimental data.

T (K)	a (Å)	error	b (Å)	error	c (Å)	error	V (Å ³)	error
100	7.367604	0.000389	9.447755	0.000974	6.817147	0.000665	474.523`	0.072
107	7.371495	0.000645	9.451592	0.003088	6.821949	0.001339	475.301	0.186
113	7.375247	0.000641	9.456141	0.003086	6.826862	0.001338	476.115	0.186
119	7.379206	0.000623	9.460782	0.002984	6.831974	0.001295	476.961	0.18
125	7.383172	0.000598	9.465656	0.002908	6.837165	0.001266	477.826	0.176
131	7.387102	0.000584	9.469931	0.002841	6.842484	0.001247	478.668	0.172
137	7.391238	0.000574	9.474752	0.002816	6.847878	0.001232	479.558	0.171
143	7.395613	0.000581	9.479299	0.00283	6.853774	0.001233	480.485	0.172
149	7.399932	0.000583	9.483052	0.002744	6.859961	0.001153	481.39	0.165
155	7.404373	0.000582	9.488679	0.002697	6.865695	0.001135	482.368	0.163
161	7.408688	0.000587	9.494147	0.002698	6.87132	0.00115	483.323	0.164
167	7.413356	0.000583	9.50034	0.002662	6.877565	0.001185	484.383	0.164
173	7.417736	0.000582	9.506635	0.002572	6.883277	0.001226	485.393	0.162
179	7.421371	0.000575	9.515035	0.002527	6.889902	0.001326	486.528	0.164
185	7.424926	0.00052	9.522322	0.002422	6.896476	0.001247	487.598	0.156
191	7.42858	0.000534	9.528765	0.002587	6.902442	0.001306	488.591	0.165
197	7.432215	0.000556	9.53513	0.002754	6.909028	0.001368	489.623	0.175
203	7.435473	0.000572	9.541116	0.002834	6.915467	0.001406	490.602	0.181
209	7.439347	0.000595	9.548349	0.002959	6.922979	0.001471	491.763	0.189
215	7.444887	0.000617	9.554997	0.003068	6.92942	0.001527	492.93	0.196
221	7.448066	0.000615	9.561076	0.003033	6.937469	0.001506	494.028	0.194
227	7.453427	0.000593	9.569259	0.002943	6.945703	0.001458	495.394	0.189
233	7.459602	0.000573	9.579181	0.002843	6.955146	0.001417	496.993	0.183
239	7.464406	0.000565	9.589831	0.00269	6.965685	0.001328	498.62	0.173
245	7.46676	0.000488	9.60187	0.002363	6.979116	0.001181	500.367	0.153
251	7.466404	0.000356	9.619731	0.001501	6.994093	0.000684	502.349	0.096
257	7.469001	0.000424	9.633566	0.001791	7.006597	0.000827	504.146	0.115
263	7.471334	0.000692	9.648976	0.002621	7.018728	0.001298	505.985	0.173

References

- S1. N. I. Joukovsky, *Bull. Soc. Chim. Belges.*, 1934, **43**, 397.
- S2. J. R. Goates, J. B. Ott and A. H. Budge, *J. Phys. Chem.*, 1961, 2162.
- S3. H. M. Rietveld, *J. Appl. Crystallogr.* 1969, **2**, 65-71.
- S4. G. E. Bacon, N. A. Curry and S. A. Wilson, *Proc. R. Soc. A: Math. Phys. Engineering Sci.* 1964, **279**, 98.
- S5. A. A. Coelho, *J. Appl. Crystallogr.* 2003, **36**, 86.
- S6. G. S. Pawley, *J. Appl. Crystallogr.* 1981, **14**, 357.
- S7. Y. G. Andreev, G. S. MacGlashan, P. G. Bruce, *Phys. Rev. B: Condens. Matter Phys.* 1997, **55**, 12011.
- S8. P. S. Whitfield, *J. Appl. Crystallogr.* 2009, **42**, 134.
- S9. H. E. Maynard-Casely, R. Hodyss, M. L. Cable, T. Hoang Vu and M. Rahm, *IUCrJ*, 2016, **3**, 192.
- S10. J. P. Perdew, K. Burke and Matthias Ernzerhof, *Phys. Rev. Lett.* 1996, **77**, 3865.
- S11. N. Mardirossian and M. Head-Gordon, *Phys. Chem. Chem. Phys.* 2014, **16**, 9904.
- S12. S. Grimme, S. Ehrlich and L. Goerigk, *J. Comp. Chem.* 2011, **32**, 1456.
- S13. Gaussian 16, Revision C.01, M. J. Frisch, G. W. Trucks, H. B. Schlegel, G. E. Scuseria, M. A. Robb, J. R. Cheeseman, G. Scalmani, V. Barone, G. A. Petersson, H. Nakatsuji, X. Li, M. Caricato, A. V. Marenich, J. Bloino, B. G. Janesko, R. Gomperts, B. Mennucci, H. P. Hratchian, J. V. Ortiz, A. F. Izmaylov, J. L. Sonnenberg, D. Williams-Young, F. Ding, F. Lipparini, F. Egidi, J. Goings, B. Peng, A. Petrone, T. Henderson, D. Ranasinghe, V. G. Zakrzewski, J. Gao, N. Rega, G. Zheng, W. Liang, M. Hada, M. Ehara, K. Toyota, R. Fukuda, J. Hasegawa, M. Ishida, T. Nakajima, Y. Honda, O. Kitao, H. Nakai, T. Vreven, K. Throssell, J. A. Montgomery, Jr., J. E. Peralta, F. Ogliaro, M. J. Bearpark, J. J. Heyd, E. N. Brothers, K. N. Kudin, V. N. Staroverov, T. A. Keith, R. Kobayashi, J. Normand, K. Raghavachari, A. P. Rendell, J. C. Burant, S. S. Iyengar, J. Tomasi, M. Cossi, J. M. Millam, M. Klene, C. Adamo, R. Cammi, J. W. Ochterski, R. L. Martin, K. Morokuma, O. Farkas, J. B. Foresman, and D. J. Fox, Gaussian, Inc., Wallingford CT, 2016.
- S14. M. J. Cliffe and A. L. Goodwin, *J. Appl. Cryst.*, 2012, **45**, 1321.